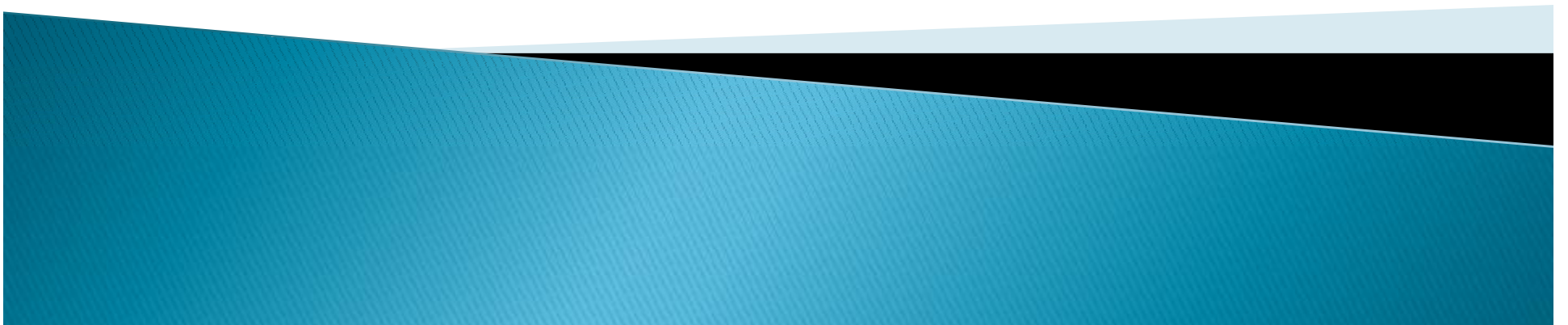


Renewable Energy Systems

EE—325



History

In **1839**, at age 19, the photovoltaic effect was experimentally demonstrated first by French physicist **Edmond Becquerel**.

In **1873** **Willoughby Smith** first described the "Effect of Light on Selenium during the passage of an Electric Current" in a 20 February 1873 issue of **Nature**.

In **1883** **Charles Fritts** built the first solid state photovoltaic cell by coating the semiconductor **selenium** with a thin layer of gold to form the junctions; the device was only around **1%** efficient.

Selenium is a chemical element with the symbol **Se** and atomic number **34**. Selenium is a semiconductor and is used in photocells.

History

1888—Russian physicist **Aleksandr Stoletov** built the first cell based on the outer photoelectric effect.

1905—**Albert Einstein** proposed a new quantum theory of light and explained the photoelectric effect, for which he received the Nobel Prize in Physics in **1921**.

1946—**Russell Ohl** patented the modern junction semiconductor solar cell, while working on the invention of transistors.

1954—**The first practical photovoltaic cell was publicly demonstrated at Bell Laboratories. The inventors were Calvin Souther Fuller, Daryl Chapin and Gerald Pearson. Solar Cell Efficiency =5%.**

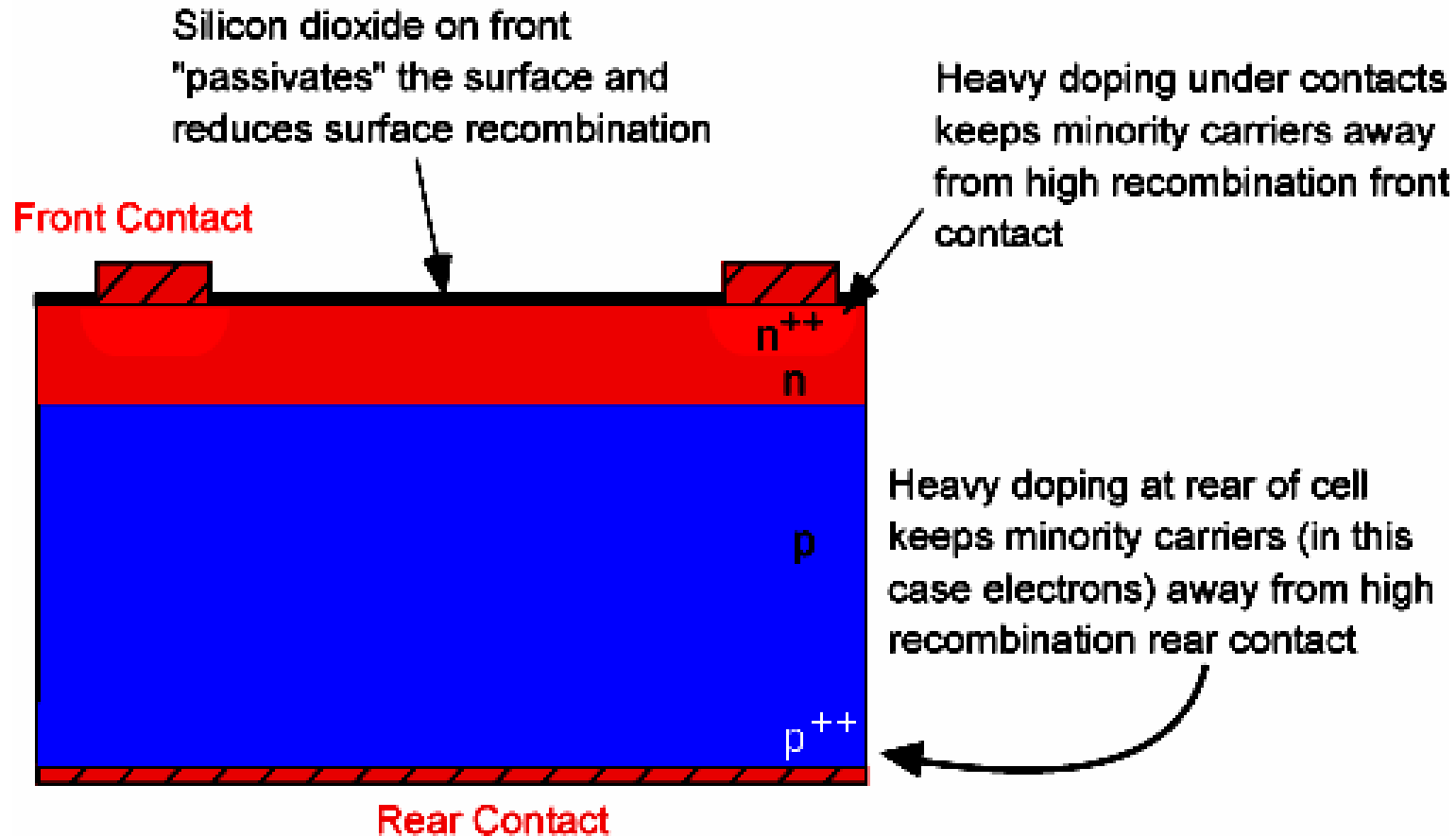
1957—Egyptian engineer **Muhammad M. Atalla** develops the process of silicon surface passivation by thermal oxidation at Bell Laboratories. The surface passivation process has since been critical to solar cell efficiency.

1958—Solar cells gained prominence with their incorporation onto the **Vanguard I** satellite.

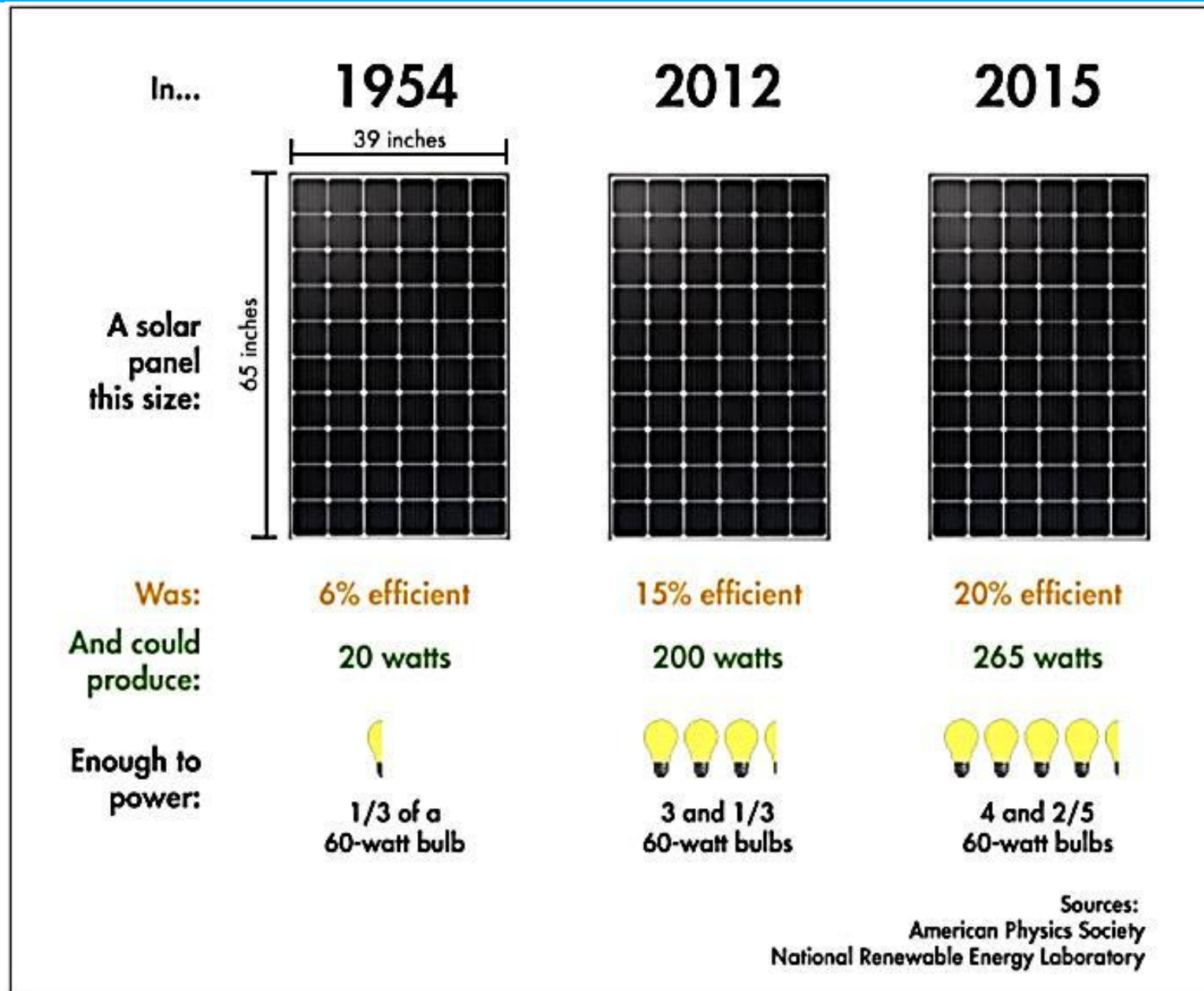
Silicon Surface Passivation

Surface passivation is the process by which the semiconductor surface is purified inert and does not change semiconductor properties as a result of interaction with air or other materials in contact with the surface or edge of the crystal.

Passivation involves creation of an outer layer of shield material.

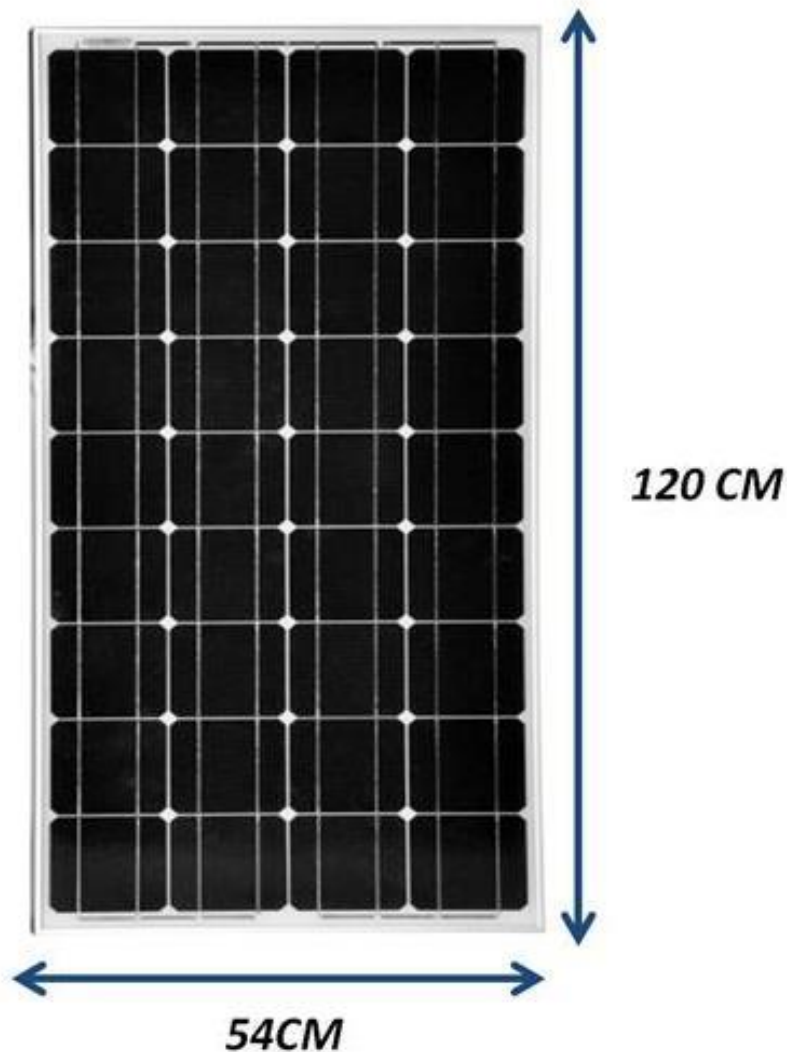


History



How to Read a Solar Panel

SOLAR PANEL 100W

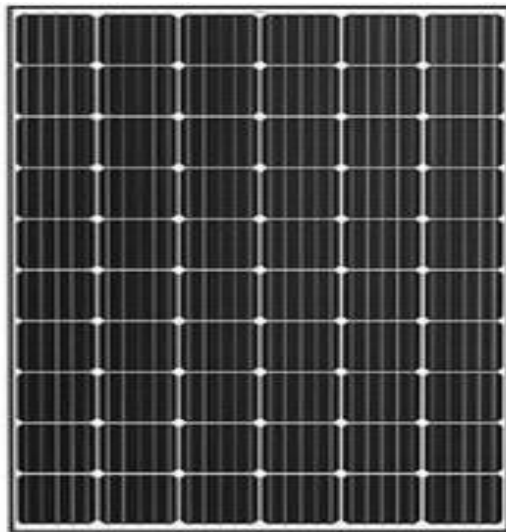


MODEL	PVM-100 (Monocrystalline)
POWER	100W
NUMBER,SIZE OF CELLS	36 Pcs / 4*9
POWER TOLERANCE	± 3%
VOLTAGE	18.17V
CURRENT	5.51A
OPEN VOLTAGE	21.6V
SHORT CURRENT	6.06A
MAXIMUM VOLTAGE	1000V
DIODE	2 by-pass
SIZE	-
WEIGHT	7.8Kg
TEMPERATURE RANGE	-40/+85°C
GUARANTEE	10 YEAR GUARANTEE OF 90% POWER 25 YEARS 80% POWER

Average Efficiency of Different Solar Panels



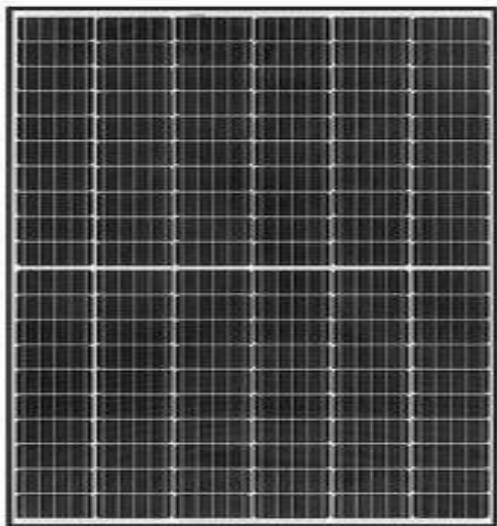
60 cell - Poly
16 - 17%



60 cell - Mono PERC
17 - 19%



Shingled cells - Mono
17 - 19%



120 cell - Half-cut mono
18 - 20%

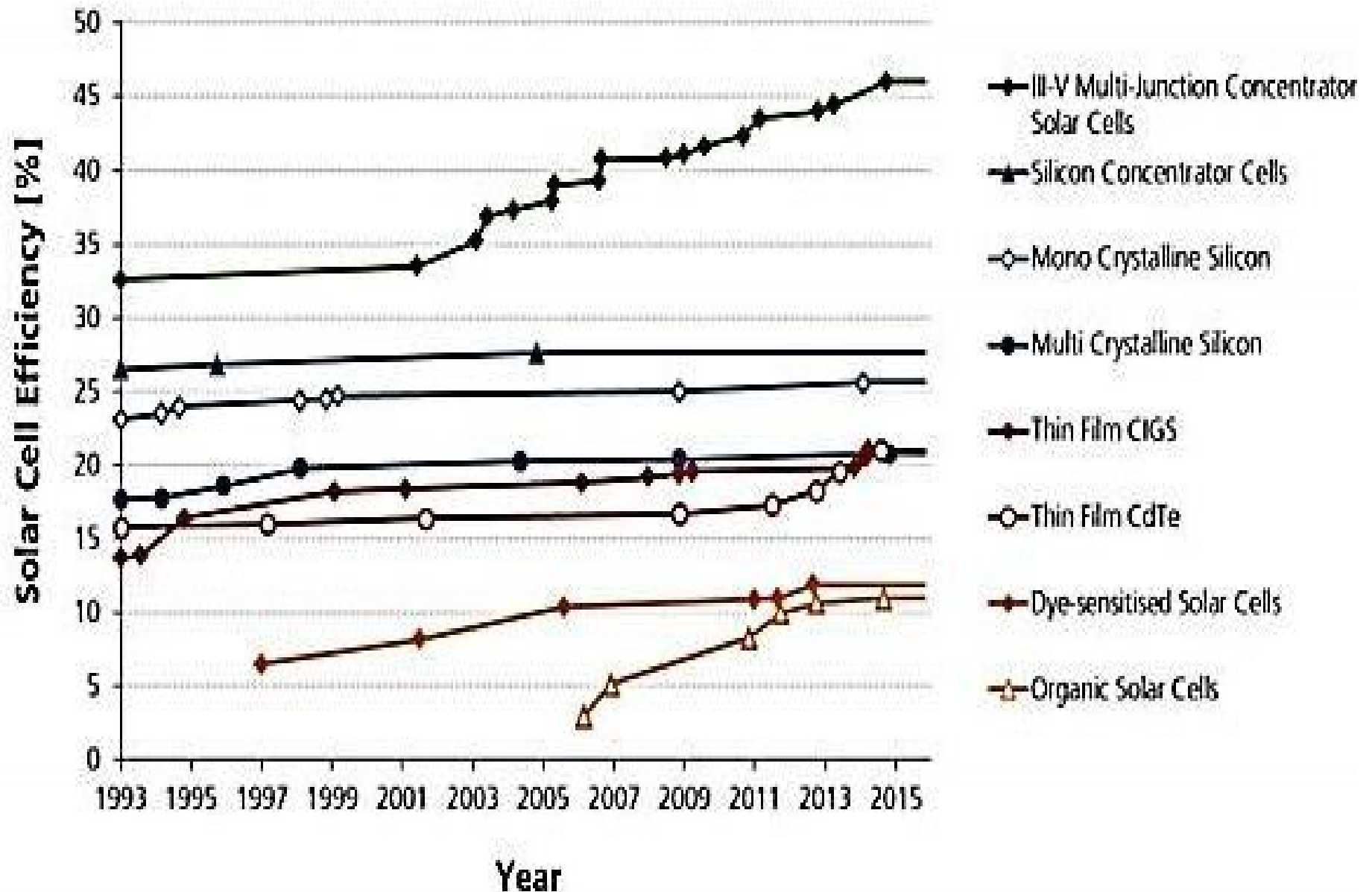


60 cell - Multi busbar
18 - 20%



60 or 96 cell - IBC
20 - 22%

Development of Laboratory Solar Cell Efficiencies



Data: Solar Cell Efficiency Tables (Versions 1-46), Progress in Photovoltaics: Research and Applications, 1993-2015. Graph: Simon Phillips, Fraunhofer ISE 2015

Semiconductors for solar application: Semiconductors as materials for solar cells, Carrier concentration and distribution, generation-recombination processes, Continuity Equations.

Consideration of the Photodiode: Method of Function of the Solar Cell, Photocurrent, Characteristic Curve and Characteristic Dimensions, Electrical Description of Real Solar Cells, Considering Efficiency, High Efficiency Cells.

3.1.1 Bohr's Atomic Model

According to Bohr's atomic model, an atom consists of a nucleus and a shell. The **nucleus** contains **protons and neutrons** whereas the **shell** contains **electrons**, which orbit the nucleus. The **value** of the **elementary charge** is $1.6 \times 10^{-19} \text{ C}$. The simplest atom, **hydrogen atom**, has the atomic number 1 and thus has only one proton in the nucleus and one electron in the shell. Bohr recognized that electrons can only circulate in very particular paths (so-called "shells") about the nucleus.

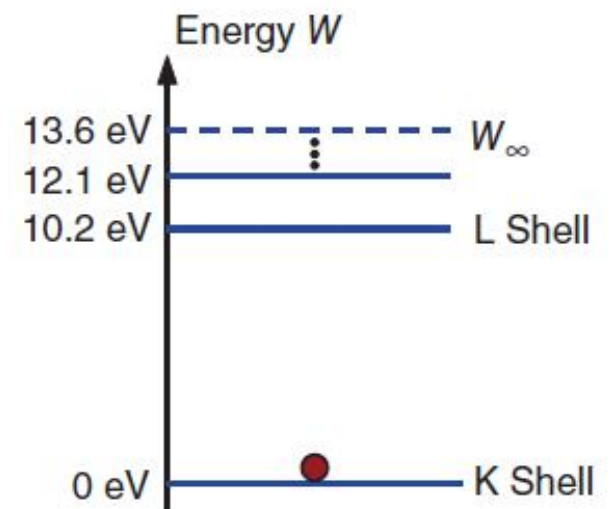
Bohr's First Postulate:

There are only certain discrete shells permitted for an electron.

Each of these shells stands for a respective energy state of the electron. The shells are designated with the letters of K, L, M, and so on.

Initially, the electron is situated on the **K shell**. If the electron is moved to the **L shell** then **energy of 10.2 eV** (electron volts) is necessary.

In order to separate the electron completely from the the so-called **ionizing energy** W_{∞} of **13.6 eV** is required.



3.1.1 Bohr's Atomic Model

Bohr's Second Postulate:

The transfer of an electron from one shell to another occurs under the emission or absorption of electromagnetic radiation.

The **frequency** f of this radiation is thus determined by the following equation:

$$\Delta W = |W_2 - W_1| = h \cdot f \quad (3.1)$$

With W_1 : energy before the transfer
 W_2 : energy after the transfer
 h : Planck's constant; $h=6.62607015 \times 10^{-34}$ J·s

In order to determine the **wavelength** λ from the frequency f the following equation is used:

$$\lambda = \frac{c_0}{f}, \quad c_0 = 299.792 \text{ km/s} \approx 3 \cdot 10^8 \text{ m/s} \quad (3.2)$$

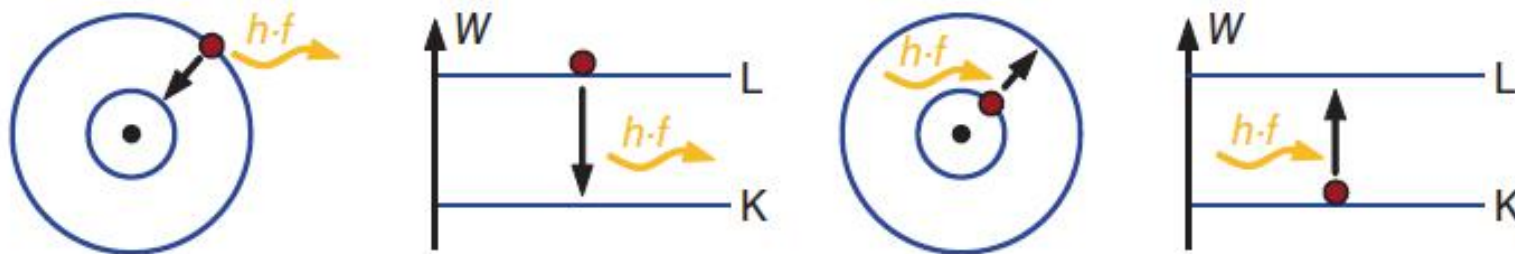
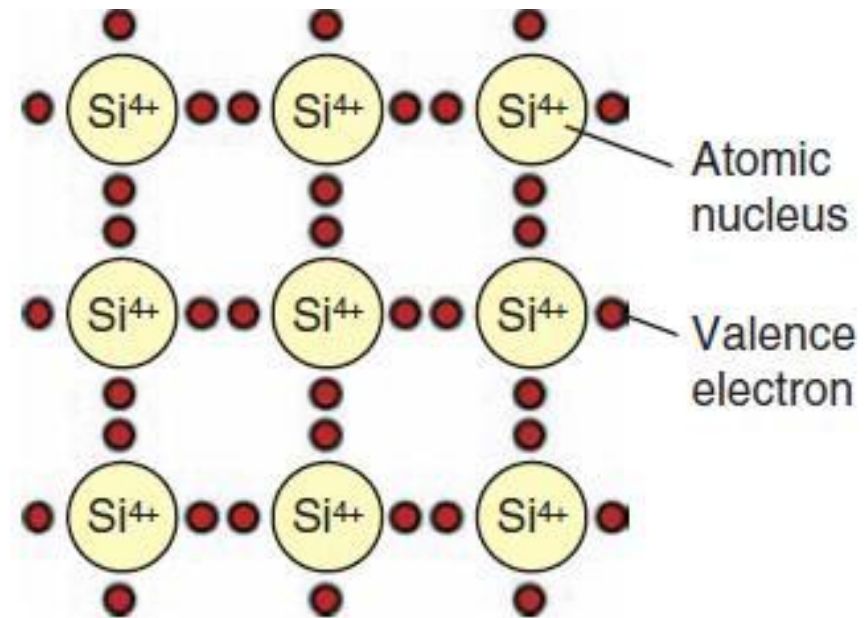
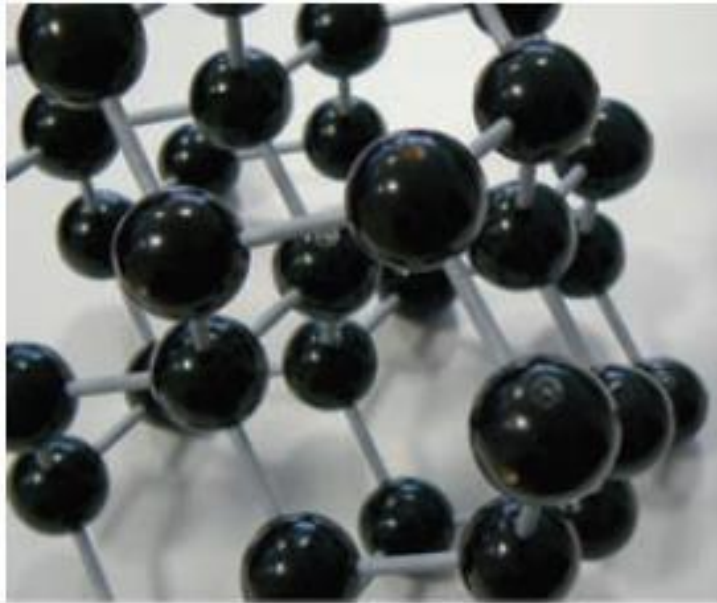


Figure 3.2 Schematic depiction of the emission (left) and absorption (right) of light

3.1.3 Structure of the Silicon Crystal

When the electrons of neighboring atoms make fixed connections, then a regular lattice structure can be formed. Such a structure is called a **crystal**.



3.1.4 Compound Semiconductors

It is possible to combine elements of different main groups. A well-known representative is the compound **gallium-arsenide (GaAs)** that can ensure high efficiencies in solar cells. It consists of trivalent gallium and pentavalent arsenic atoms and is thus called a **III/V-semiconductor**.

Figure 3.4 shows the structure so that the result is again the especially stable noble gas configuration.

Besides the III/V-semiconductor, the **II/VI-semiconductors** are also of possible; Figure 3.4 shows this in the example of cadmium-telluride (CdTe).

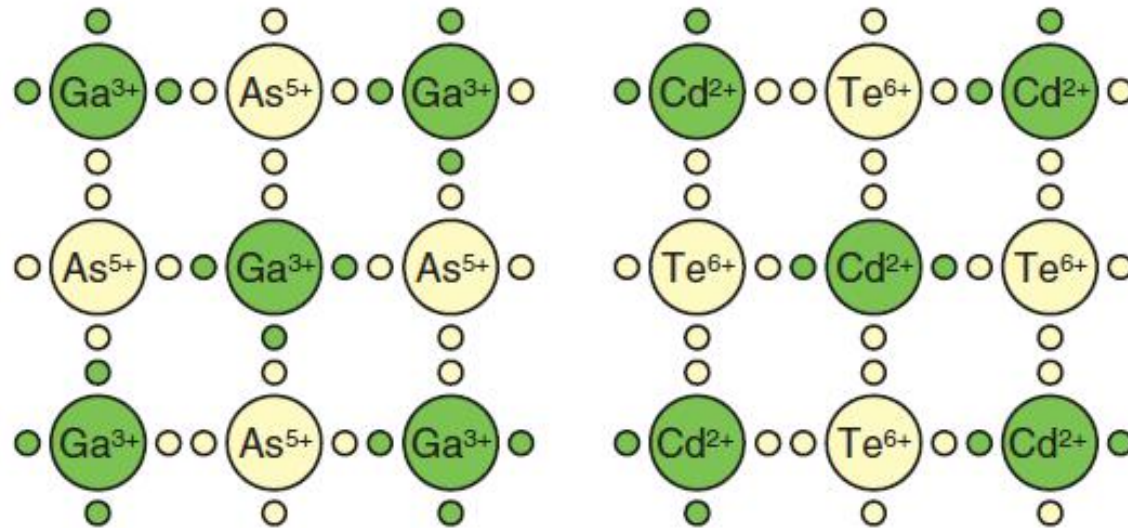


Figure 3.4 Lattice of compound semiconductors of the example GaAs and CdTe

3.2 Band Model of the Semiconductor

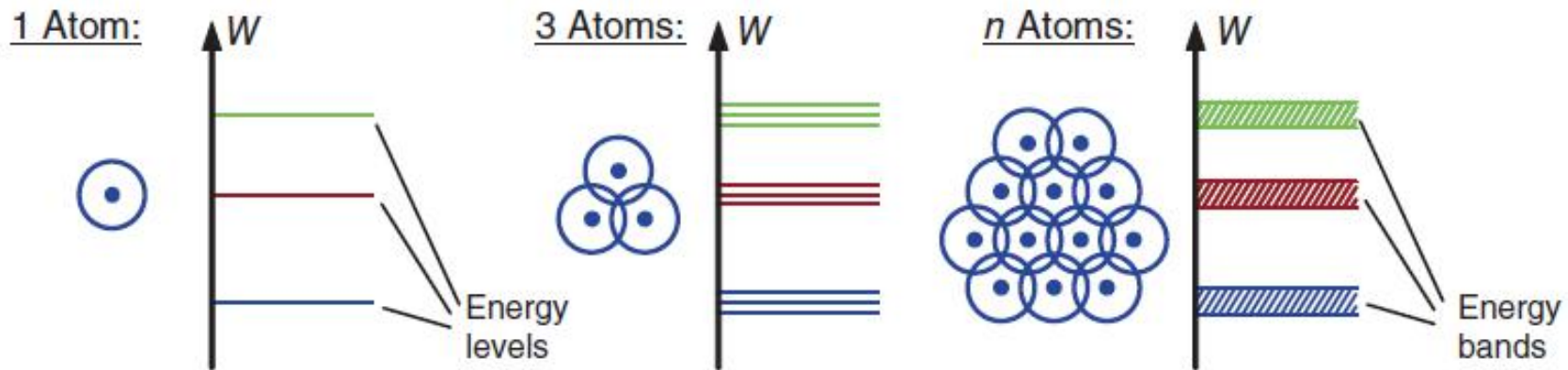


Figure 3.5 Origin of the energy bands in a semiconductor crystal: the coupling of the atoms leads to a spreading of the energy levels. For $n \rightarrow \infty$ this results in continuous energy bands

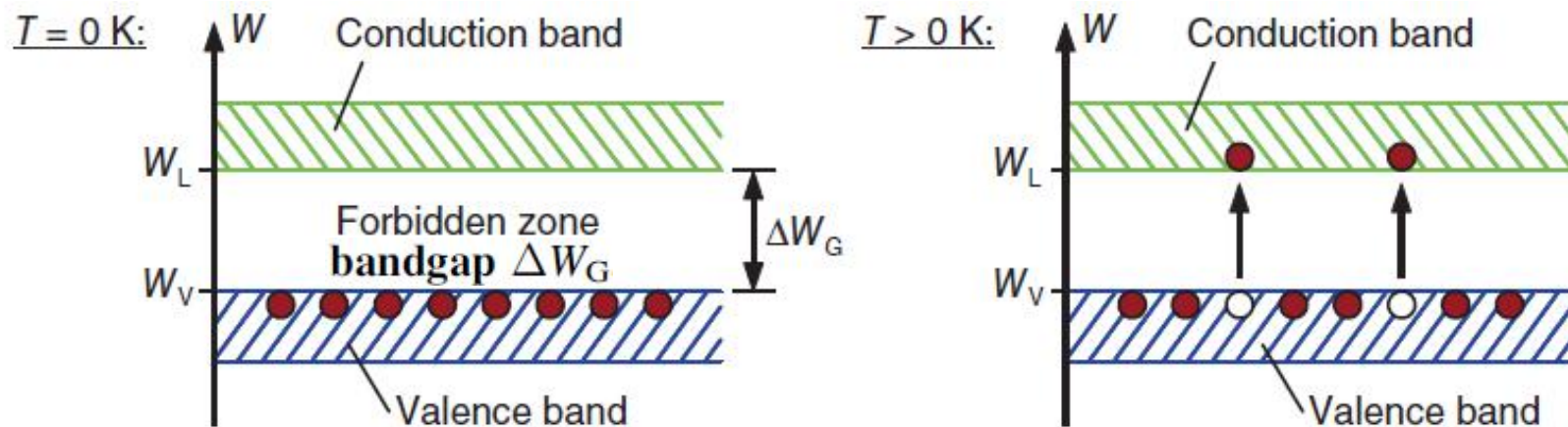


Figure 3.6 Valence and conduction bands for silicon: With rising temperatures individual electrons rise into the conduction band

3.2.2 Differences in Insulators, Semiconductors and Conductors

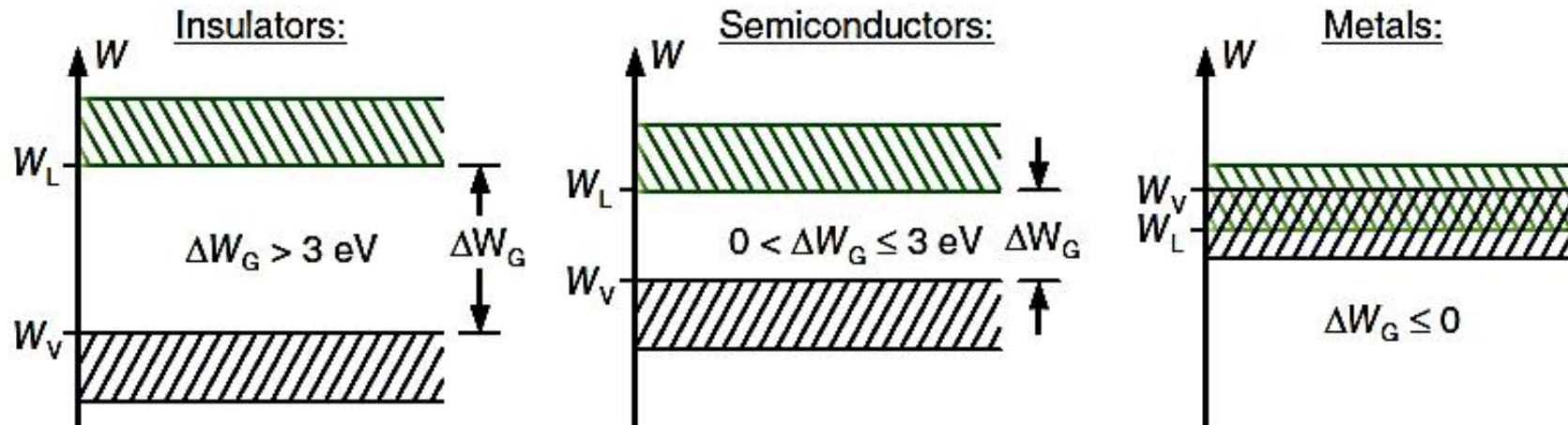


Figure 3.7 Depiction of energy bands of insulators, semiconductors and metals

Table 3.2 Comparison of the bandgaps of various materials

Material	Type of material	Bandgap ΔW_G (eV)
Diamond	Insulator	7.3
Gallium arsenide	Semiconductor	1.42
Silicon	Semiconductor	1.12
Germanium	Semiconductor	0.7

3.4 Doping of Semiconductors

Semiconductors are **poor electrical conductors**. They have achieved their particular importance in that their conductivity can be influenced in a targeted manner. For this purpose one introduces foreign atoms into the semiconductor crystal (**doping**).

Two of the most important materials **Silicon** can be doped with, are **Boron** (3 valence electrons = 3-valent) (**P—Type Material**) and **Phosphorus** (5 valence electrons = 5-valent) (**N—Type Material**).

3.4.1 N—Doping

3.4.2 P—Doping

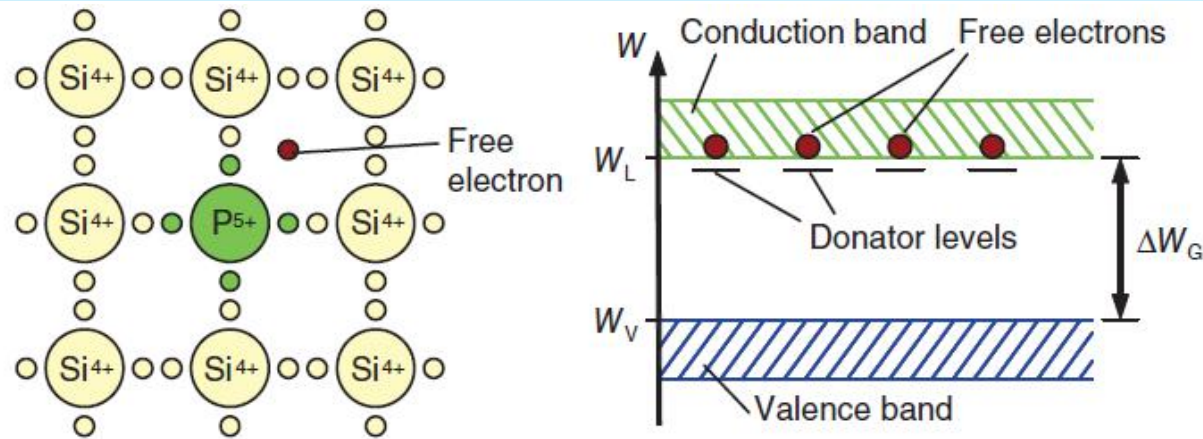


Figure 3.12 n-Doping of semiconductors; one of the five valence electrons of the phosphorous atom is not necessary for the bond and is therefore available as a free electron. Because of the doping there is a new energy level in the band diagram just below the conduction band edge

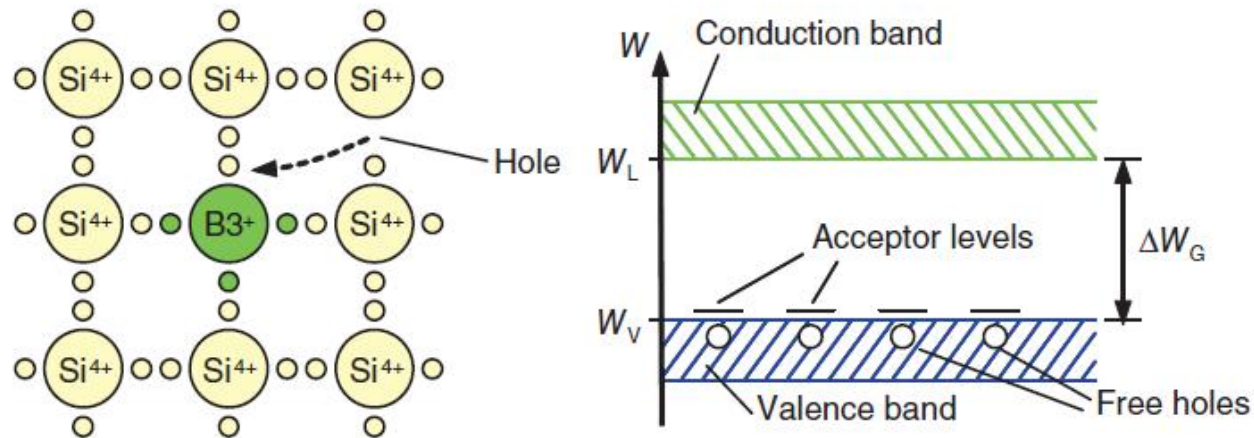
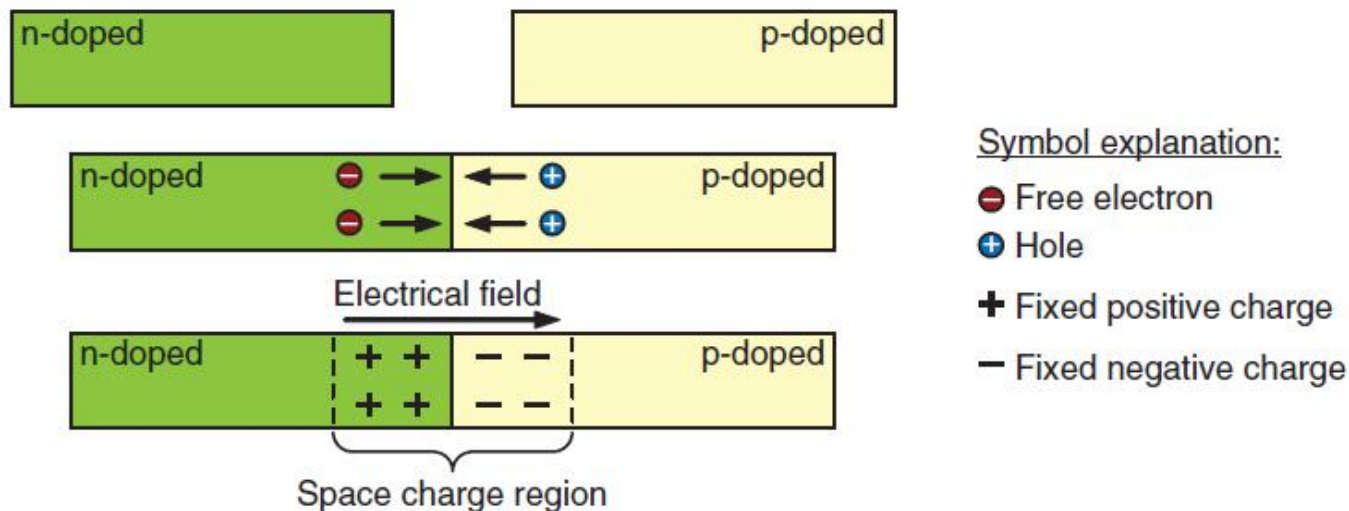


Figure 3.13 Example of p-doping of a silicon crystal with a boron atom: one of the four links remains open as the boron atom can only offer three valence electrons. A neighboring electron moves into this binding and thus “generates” a hole

3.5 The P—N Junction

Figure 3.14 shows the principle processes in a P-N junction. Both **regions are electrically neutral**. Thus, on the left side, the number of free electrons is equal to the number of fixed positive donor atoms. Let us now assume that both regions have just been combined. On the n-side there is a surplus of free electrons. These diffuse due to the **concentration gradient** from the **diffusion current** to the right into the p-doped region, and there they re-combine with the holes. A new balance is built up in which **diffusion and field current cancel each other** and a **space charge region** exists at the p-n junction. (also known as depletion region)



3.6 Interaction of Light and Semiconductors

3.6.1 Phenomenon of Light Absorption

We learned of the effect of light absorption on individual atoms when discussing the Bohr's atomic model (see Section 3.1.1). The behavior of the semiconductor is similar. In place of the individual energy levels, however, the bandgap ΔW_G is decisive here for the absorption behavior.

3.6.1 Phenomenon of Light Absorption

Incident light photons lift individual electrons from the valence into the conduction band. In order to trigger this effect, the energy W_{Ph} of the photons must be greater than the bandgap:

$$W_{\text{Ph}} = h \cdot f = \Delta W_G$$

The path of the **irradiance (light rays)** in the absorbing material can be described as,

$$E(x) = E_1 \cdot e^{-\alpha \cdot x}$$

E_1 : irradiance at $x = 0$

α : absorption coefficient

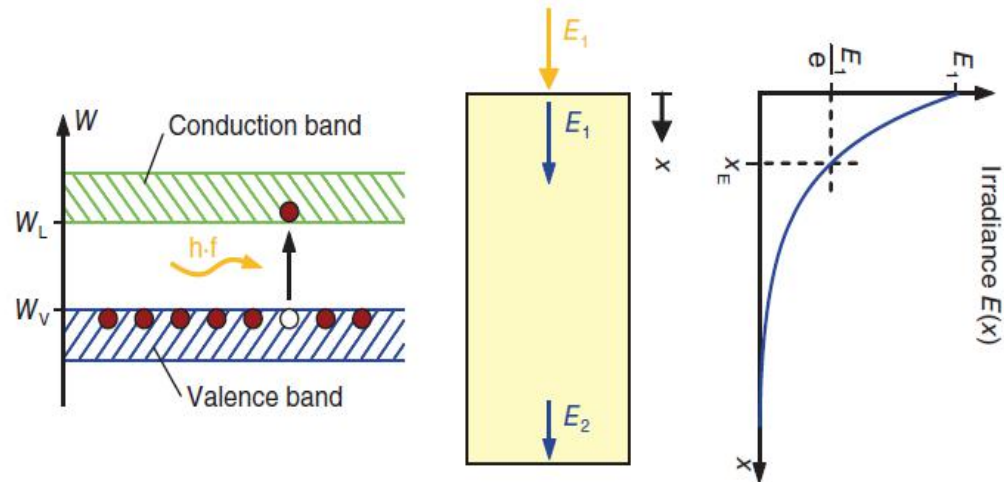


Figure 3.19 Principle of light absorption in the semiconductor. (Left); the photon is absorbed only with sufficient light energy and an electron is raised into the conduction band. (Right); incidental light radiation into a semiconductor crystal: Due to absorption in the material the light intensity sinks with increasing penetration depth

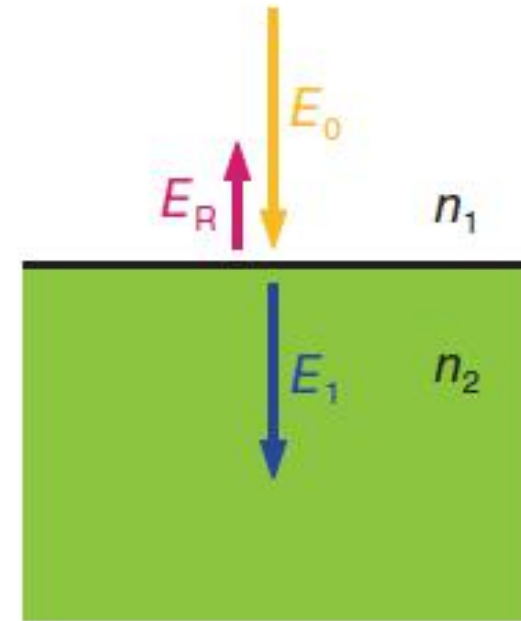
The **absorption coefficient** α indicates the absorption “ability” of the material. Another term, the **penetration depth x_p** , describes the light path the intensity has decayed by the $1/e$ times (thus approx. 37%).

$$x_p = \frac{1}{\alpha}$$

3.6.2 Light Reflection on Surfaces

3.6.2.1 Reflection Factor

Consider two materials with different *refractive indices* n_1 and n_2 . The **refractive index** n of a material indicates by which factor the speed of light is reduced compared to its speed in a vacuum: $n=c_0/c$. If the ray of light falls on an interface between two materials then *reflection* is the result. The strength of the reflection is given by the **reflection factor** R .



$$R = \frac{E_R}{E_0}$$

E_0 : incident irradiance

E_R : reflected irradiance

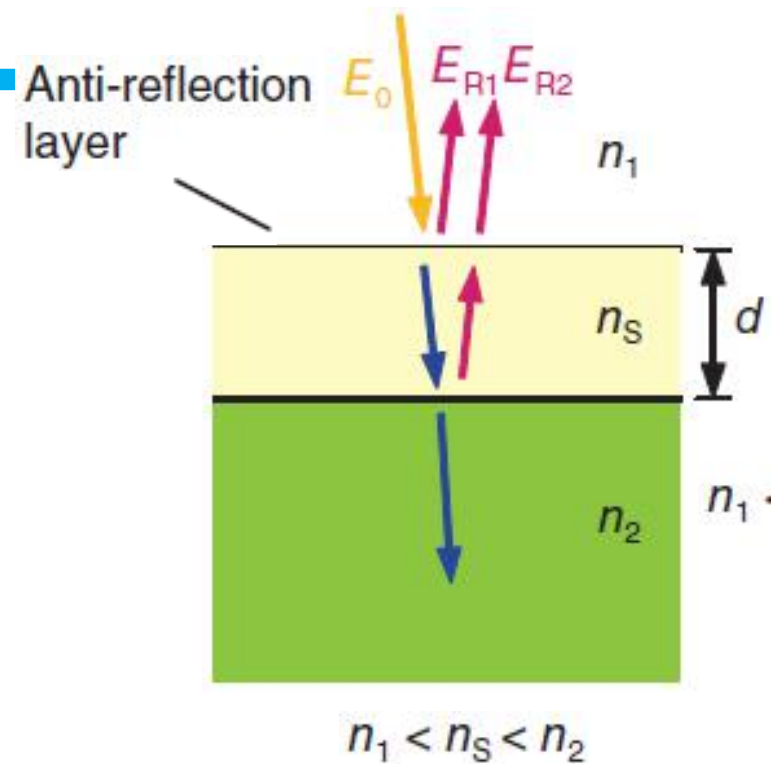
For vertical incidental radiation the reflection factor is calculated according to the following equation:

$$R = \left(\frac{n_1 - n_2}{n_1 + n_2} \right)^2$$

3.6.2.2 Anti-Reflection Coating

The incidental reflection must be reduced in order to achieve a high degree of efficiency in a solar cell. A standard means of doing this is **anti-reflection coating**.

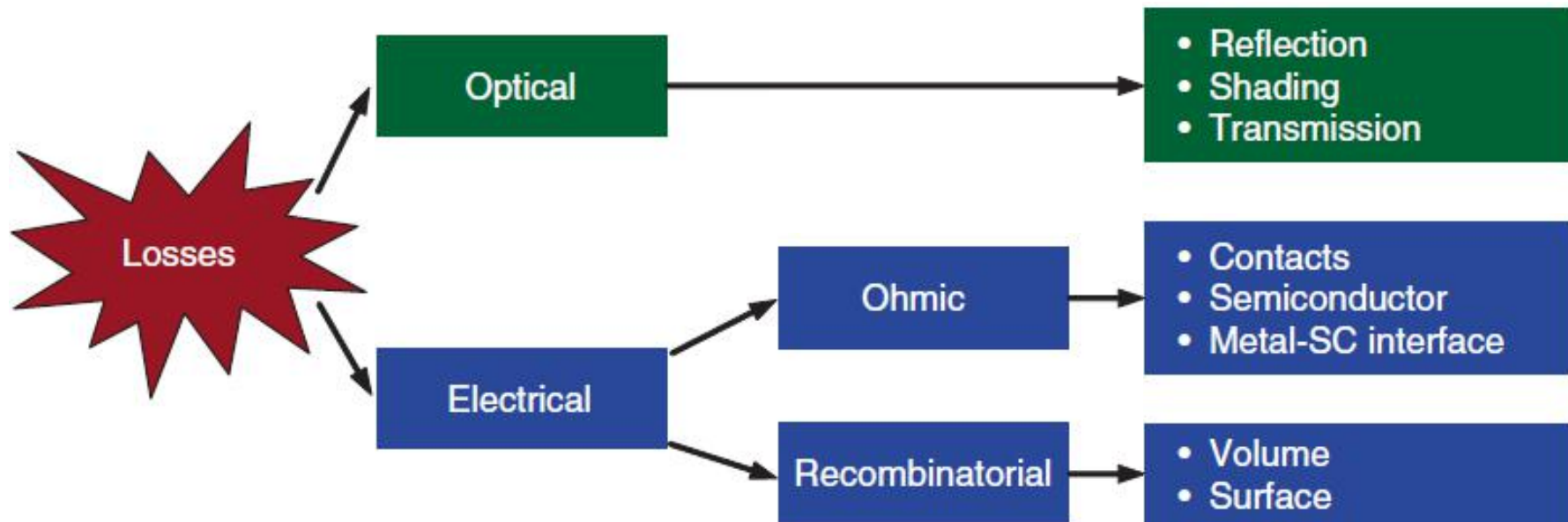
Figure shows the principle in the right-hand picture: a material of thickness d is inserted between the two media.



At the interface there is a reflective ray \mathbf{R}_1 . There is also a reflection at the transition from n_s to n_2 that appears at the surface with the strength \mathbf{R}_2 . If the layer d is made so thick that the ray 2 is displaced by 180° phase compared to ray 1 so that the reflective radiations cancel each other out due to interference.

$$d = \lambda / 4$$

4.6.3 Losses in Real Solar Cells



4.6.3.1 Optical Losses, Reflection on the Surface

As we have already seen in Chapter 3, the refractive index step of air on silicon causes a reflection of approximately 35%. **Anti-reflective coating** that lowers the average reflection of an AM 1.5 spectrum to around 10%.

A further measure is **texturing** the cell surface. The surface is etched with an acid in order to roughen it up. The results are pyramids with an angle at the top of 70.5° (Figure 4.26).

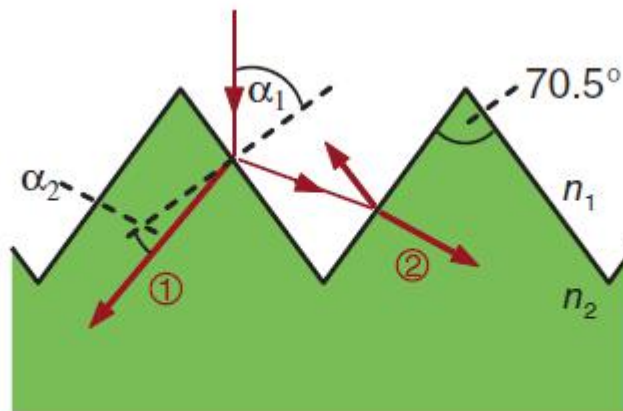


Figure 4.26 Reduction of overall reflection by means of texturing: giving light “a second chance”

4.6.3.1 Optical Losses, Reflection on the Surface

What does this texturization yield? Figure 4.26 shows how incident rays partly penetrate the cell and are partly reflected. According to the **Fresnel equations** the strength of the reflection factor R can be determined from the **angle of incidence** α_1 [29]:

$$R(\alpha) = \left(\frac{\sin(\alpha_1 - \alpha_2)}{\sin(\alpha_1 + \alpha_2)} \right)^2 \quad (4.51)$$

In this, the **exit angle** α_2 can be determined by the *law of refraction*:

$$n_1 \cdot \sin \alpha_1 = n_2 \cdot \sin \alpha_2 \quad (4.52)$$

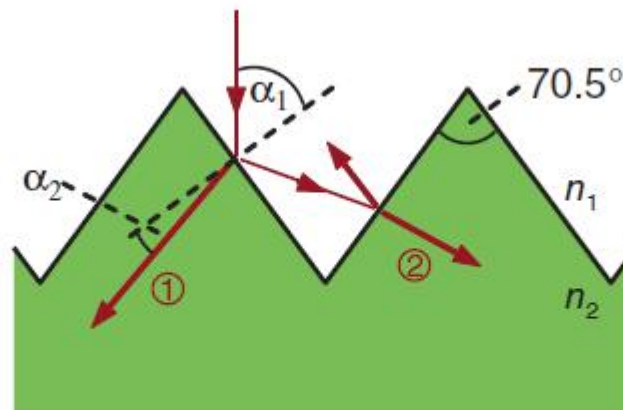


Figure 4.26 Reduction of overall reflection by means of texturing: giving light “a second chance”

4.6.3.2 Electrical Losses and Ohmic Losses

There are electrical losses in the **contact fingers** on the top side of the cell. Narrow and high contacts (in the optimum case as buried contacts) help in this. In addition, ohmic losses can occur in the **semiconductor material** as the conductivity of the doping material is limited.

Recombination Losses

The various reasons for recombination of generated charge carriers in the **semiconductor volume** have already been discussed in Section 4.2.2. Added to this in real cells are recombinations at surfaces that are created by the open bonds at the **border** of the crystal lattice.

4.7 High Efficiency Cells

4.7.1 Buried-Contact Cells

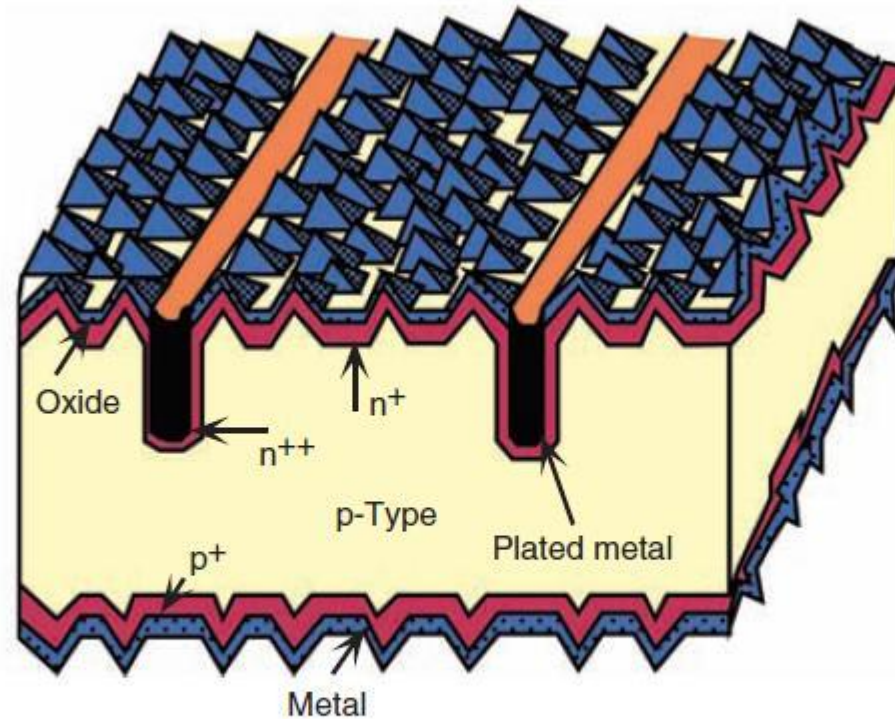


Figure 4.31 Buried contact cell (more accurately: Laser Grooved Buried Contact: LGBC cell) (reprinted with the kind permission of Martin Green)

4.7.2 Point-Contact Cell

A noticeable feature is that both the negative as well as the positive **contacts** are positioned **on the rear side of the cell** and that therefore **no shading** occurs.

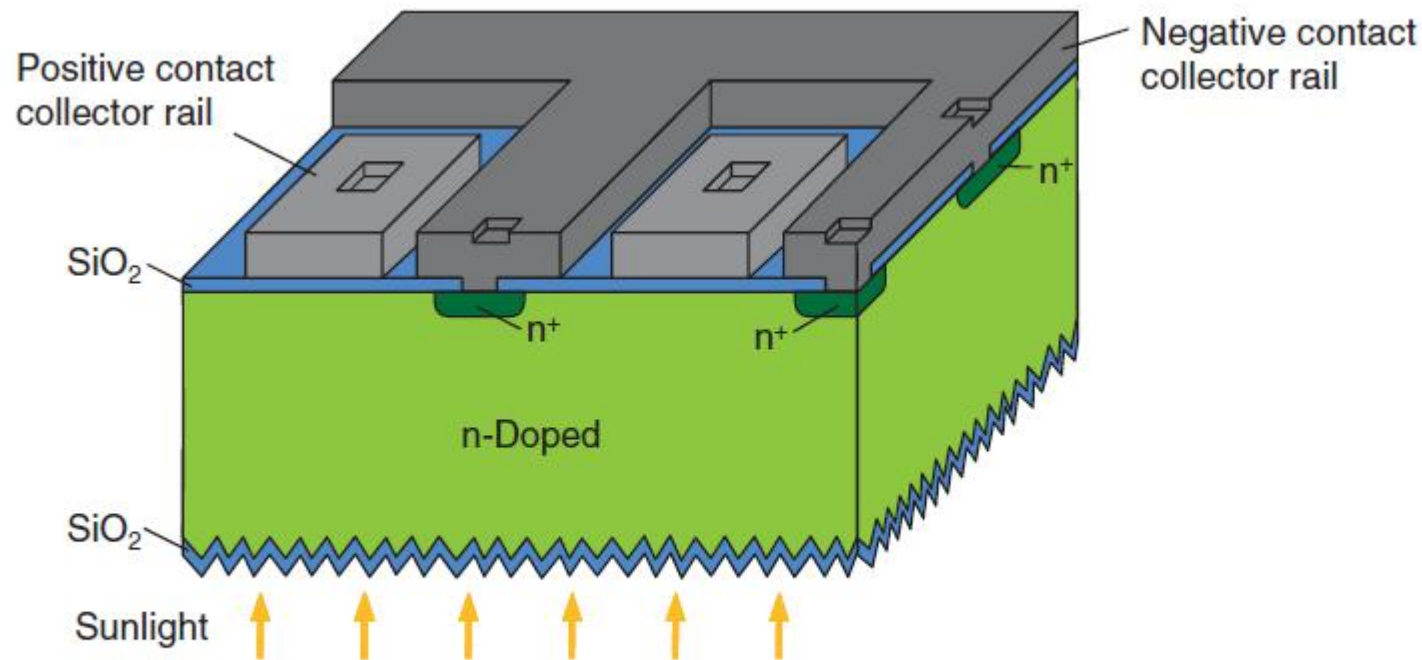


Figure 4.32 View of the point-contact cell: all contacts are positioned on the rear side of the cell and can thus be made as thick as desired [44]

4.7.3 PERL Cell (Passivated Emitter Rear Locally diffused)

The cell achieves a short circuit current of $42\text{mA}/\text{cm}^2$ and an open circuit voltage of 714 mV .

With the fill factor of 83% this results in a **record efficiency of 25%** [45,46].

Approximately 100 process steps were required for the manufacture of the record cell, which is an unacceptable effort for industrial production.

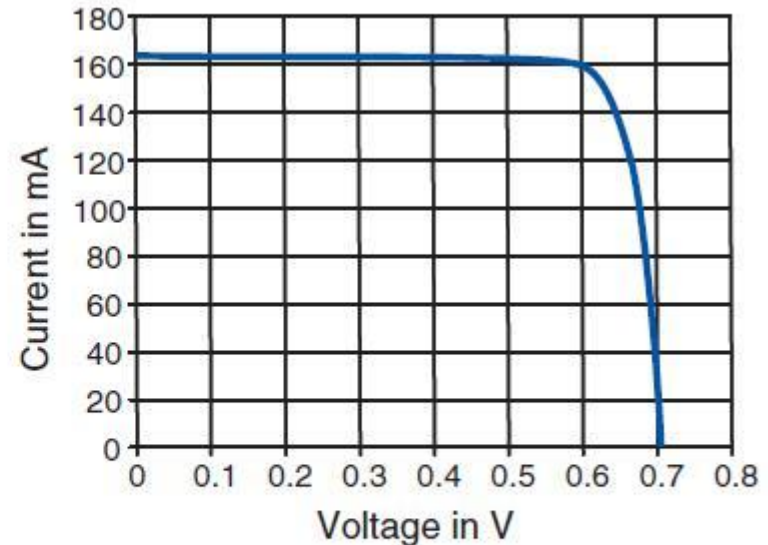
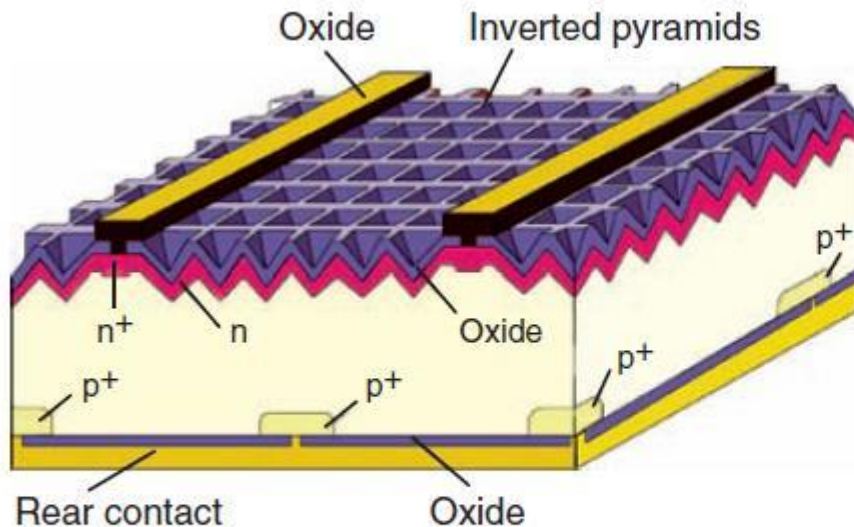


Figure 4.33 PERL cell together with I/V characteristic curve, characteristic curve to [35] (reprinted with the kind permission of Martin Green)

- 8.8 A module with 40 cells has an idealized, rectangular I-V curve with $I_{SC} = 4 \text{ A}$ and $V_{OC} = 20 \text{ V}$. If a single cell has a parallel resistance of 5 ohms and negligible series resistance, draw the I-V curve if one cell is completely shaded. What current would it deliver to a 12-volt battery (vertical I-V load at 12V)?

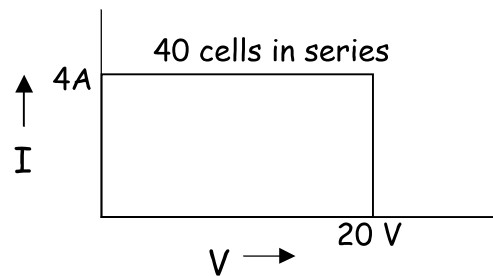


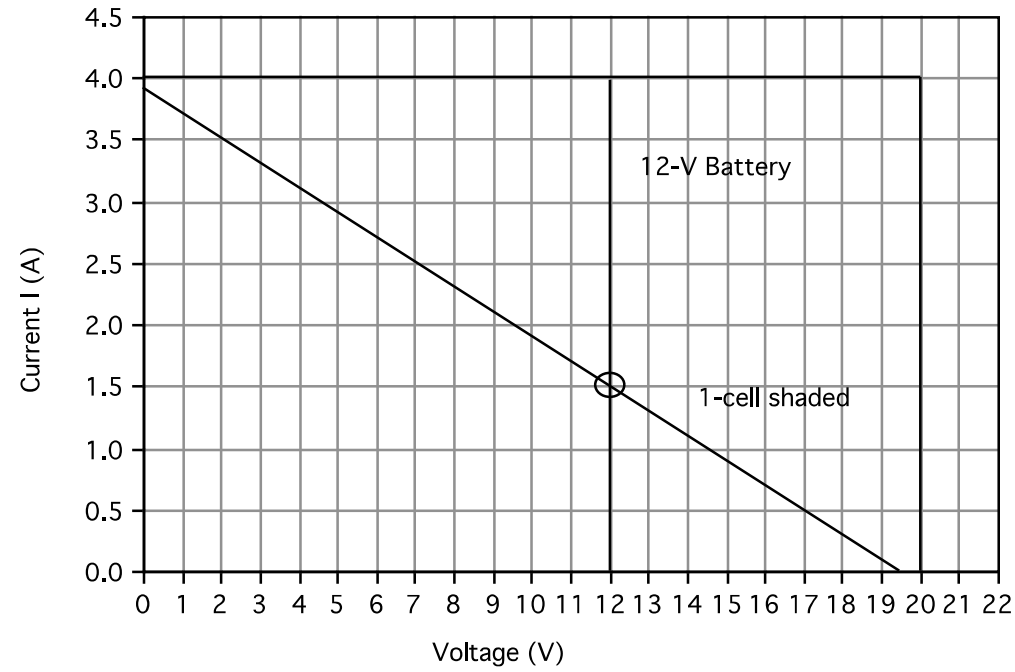
Figure P8.8

8.8 SOLN:

The voltage rise across each sunny cell is $20\text{V}/40\text{cells} = 0.5 \text{ V}$. The voltage drop across the parallel resistance in the equivalent circuit of the shaded cell is $I R = 5 I$ volts. The total voltage loss due to the single shaded cell is therefore:

$$\Delta V = 0.5 + 5 I$$

$$V = V - \Delta V = 20 - 0.5 - 5I = 19.5 - 5I$$

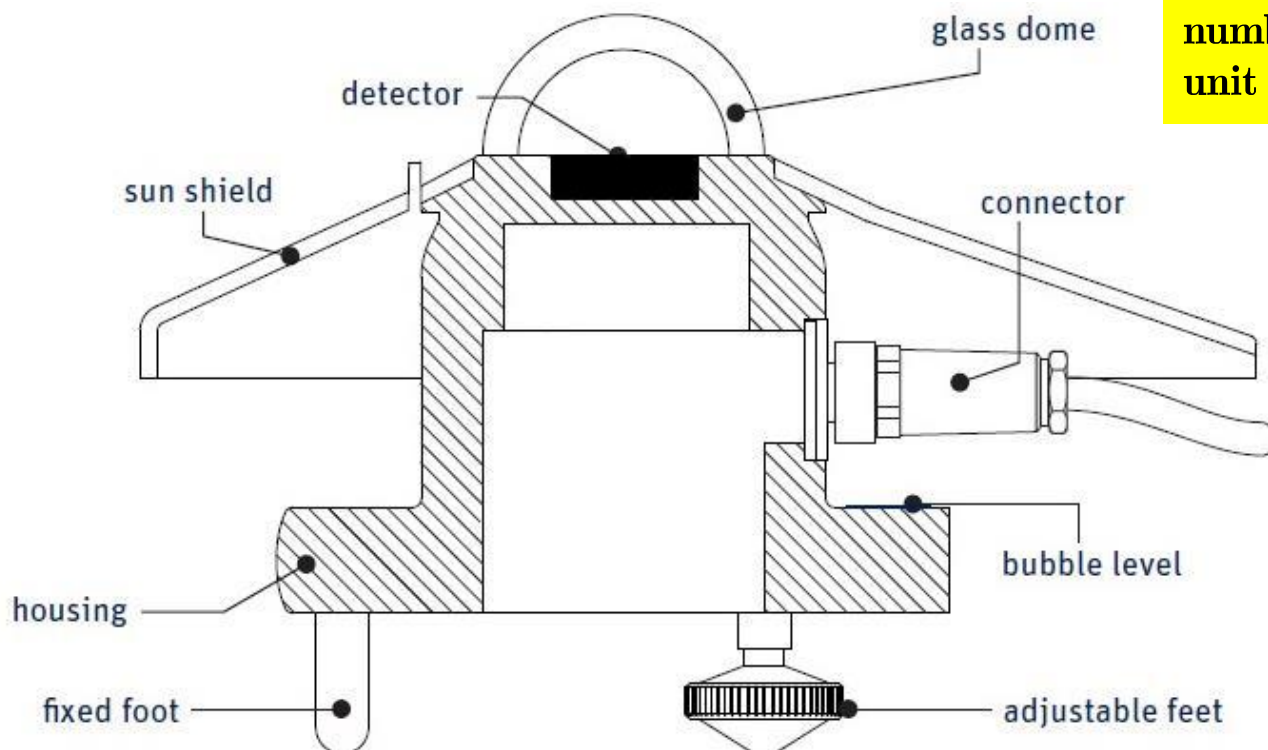


At $V = 12$ V, $I = (19.5 - 12)/5 = 1.5$ A current to the battery (instead of 4A).

Pyranometer

A **Pyranometer** is a type of actinometer used for measuring solar irradiance on a planar surface and it is designed to measure the solar **radiation flux density (W/m^2)** from the hemisphere above within a wavelength range $0.3 \mu\text{m}$ to $3 \mu\text{m}$.

Actinometers are instruments used to measure the heating power of radiation. An actinometer is a device which determines the number of photons in a beam per unit time.



Pyranometer



Photovoltaic Pyranometer

Design : A photodiode-based pyranometer is composed by a housing dome, a photodiode, and a diffuser or optical filters. The photodiode has a small surface area and acts as a sensor. The current generated by the photodiode is proportional to irradiance; an output circuit, such as a Transimpedance amplifier, generates a voltage directly proportional to the photocurrent.



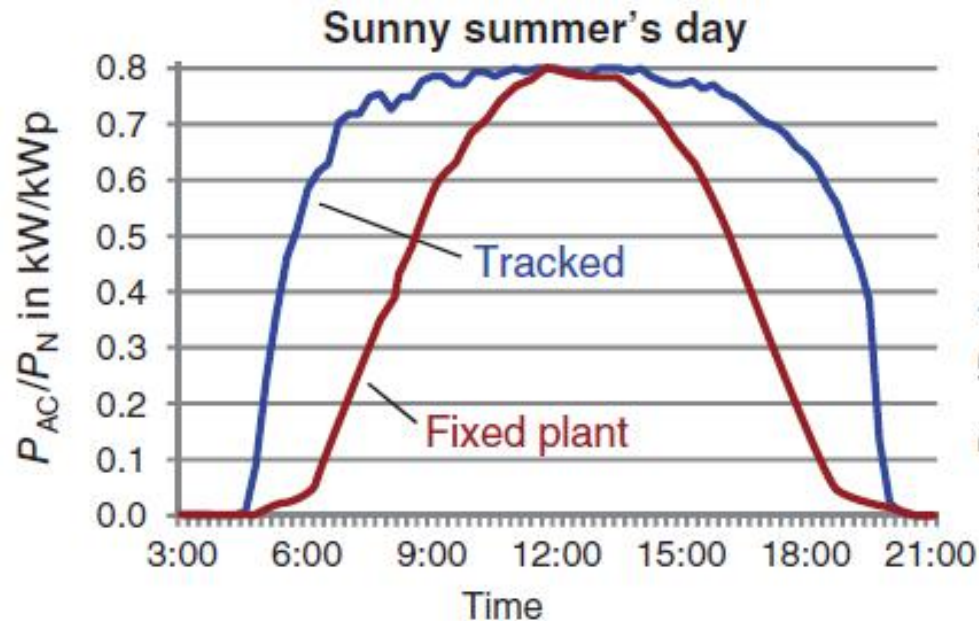
2.4.2 Radiation Estimates with Diagrams and Tables

The equations and characteristic values described are meant as an aid to understanding the features and limits of the use of solar radiation. However, simulation programs are always used today for detail planning of photovoltaic plants, and they work with refined models and detailed weather information in order to create very exact yield forecasts (see Chapter 9).

2.4.3 Yield Gain through Tracking

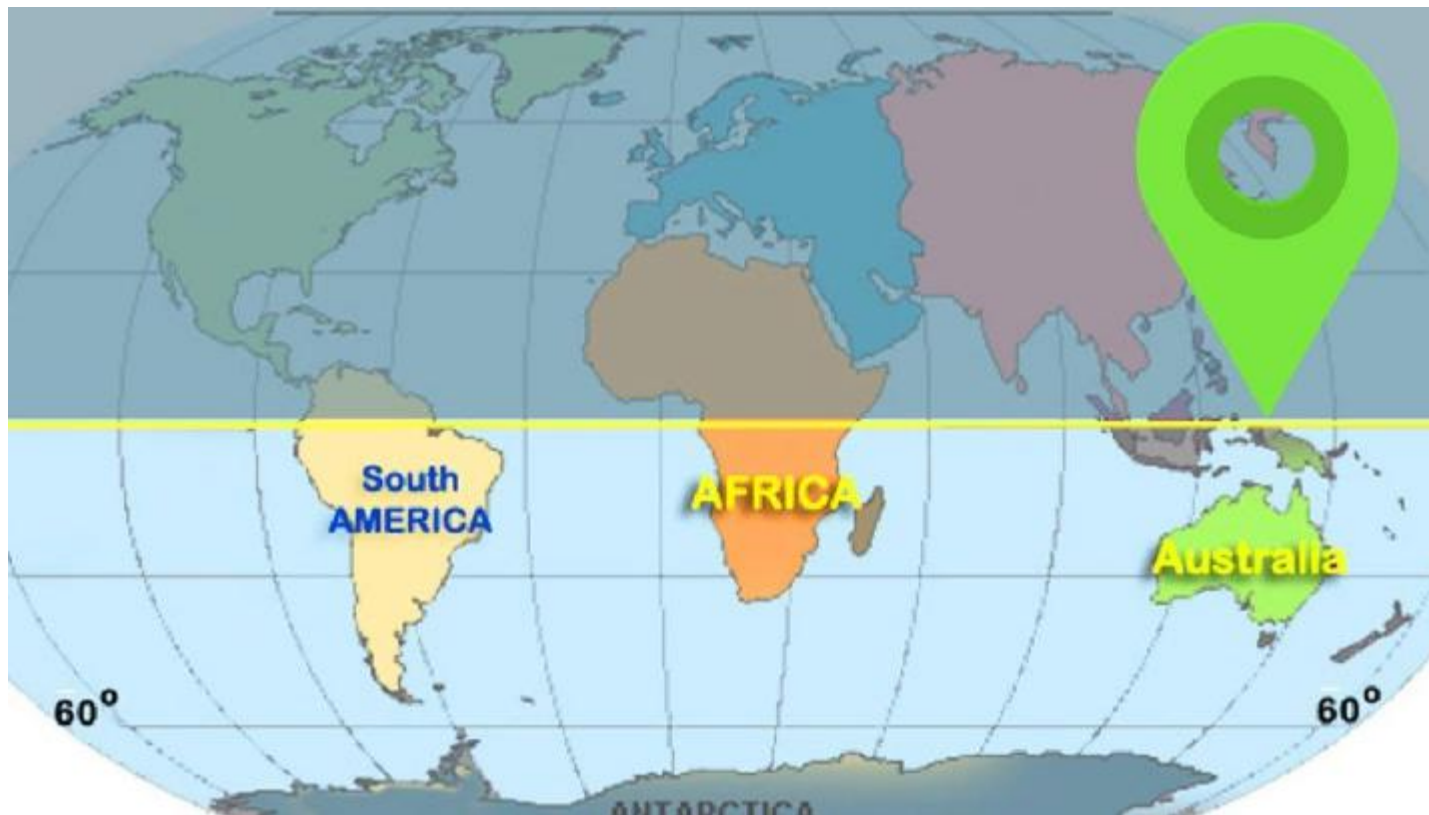
Basically, it is possible to increase the yield of a photovoltaic plant in that the solar generator actively tracks the Sun.

The tracking, however, only increases the direct radiation portion whereas the diffuse radiation remains almost the same. An example of this is shown in Figure 2.20 of the daily yield of a tracking and a fixed photovoltaic plant on two different days. On the sunny day the tracking brings an energy yield of almost 60%. In the case of the overcast day the yield of the tracking plant provides approximately 10% less than the fixed plant.

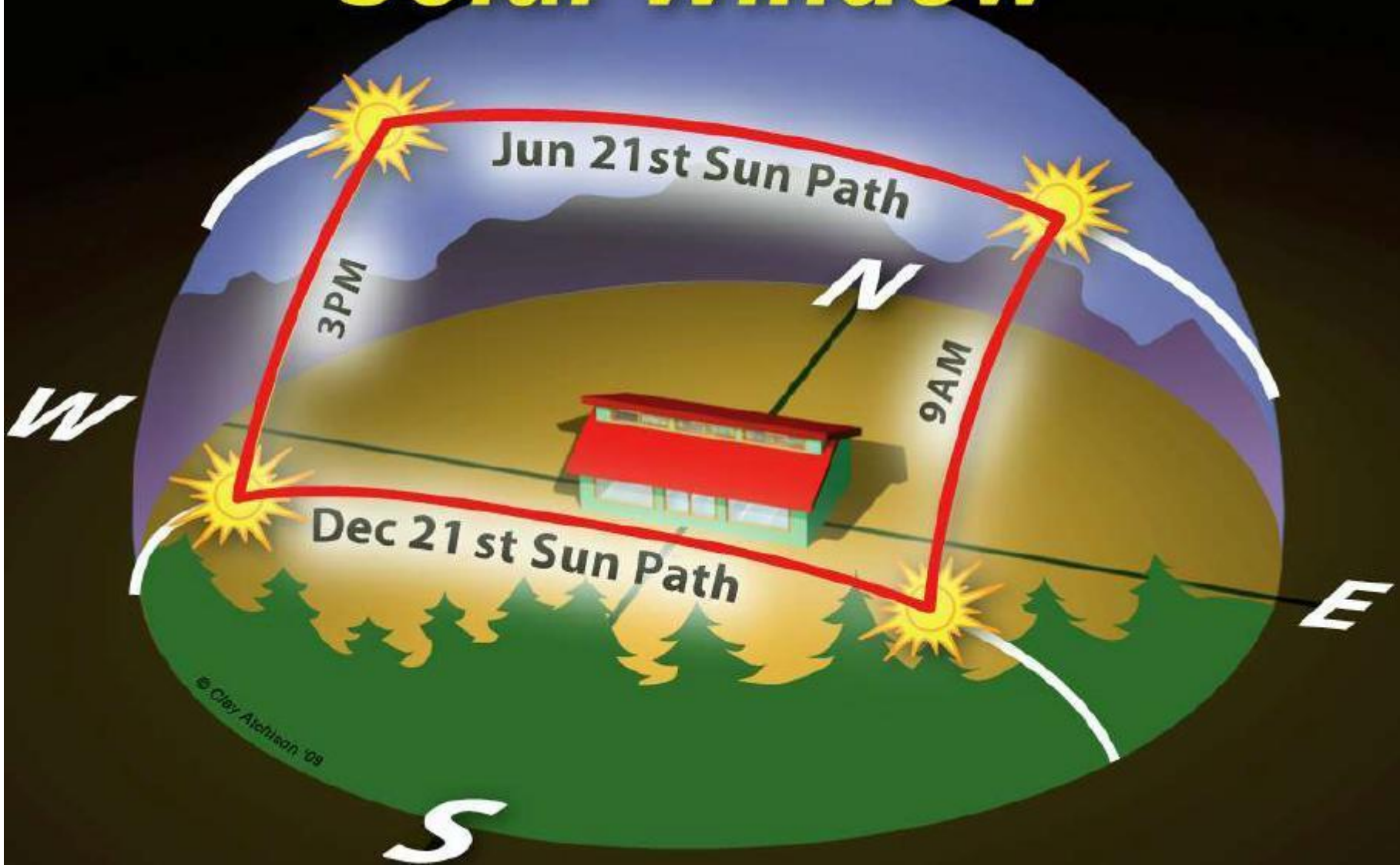


2.4.3 Yield Gain through Tracking

In **southern countries** with a high degree of direct radiation the situation is much better: Here two-axis tracking plants can achieve **more than 50%** increase in yield.



Solar Window

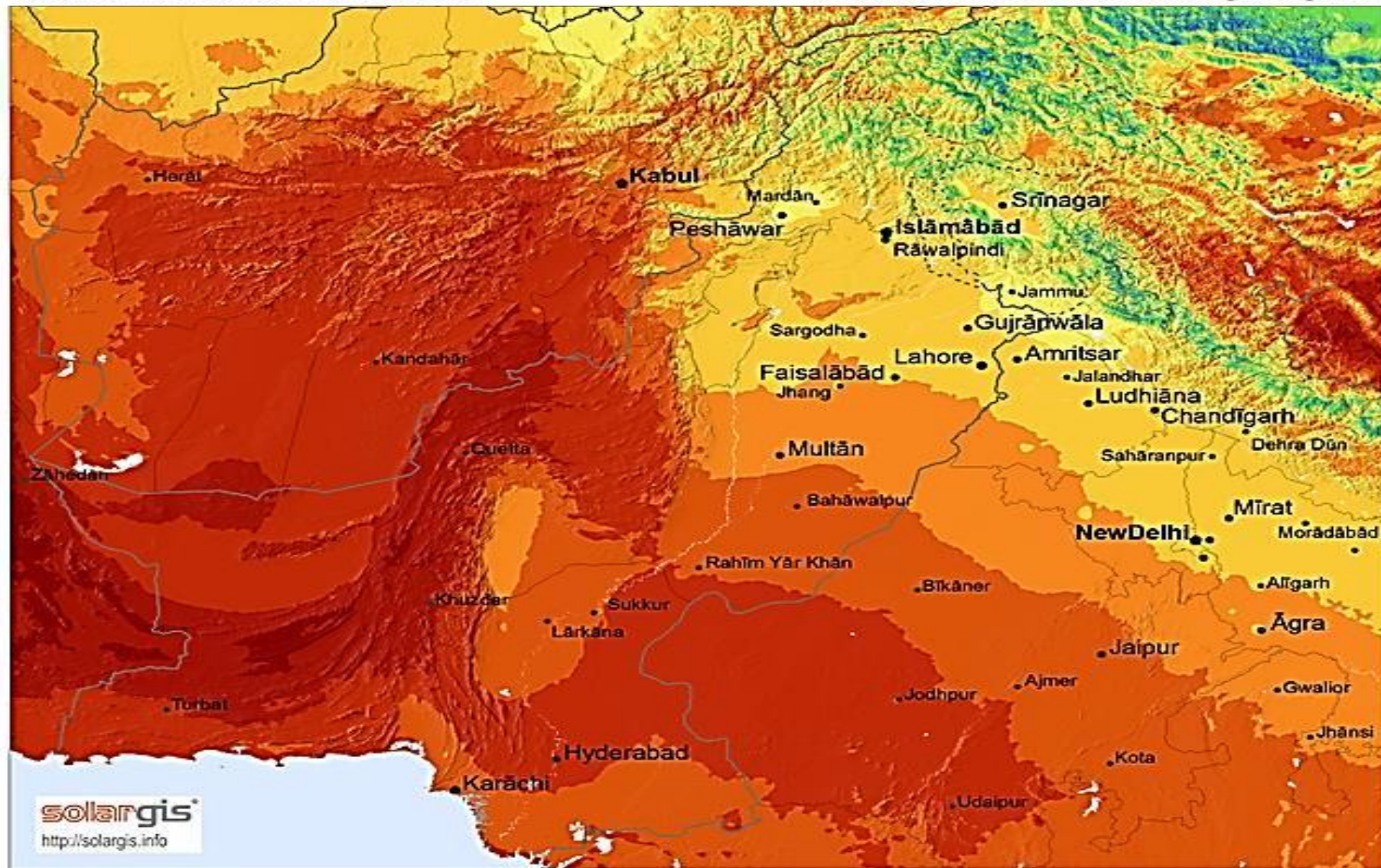


© Clay Atchison '09

Solar Potential Of Pakistan

Global Horizontal Irradiation

Pakistan And Surrounding Regions



Average annual sum (1999-2011)



0 100 200 km

SolarGIS © 2012 GeoModel Solar s.r.o.